

# Measurement of the beam intensity in a laser desorption jet-cooling mass spectrometer

Maarten G. H. Boogaarts<sup>a)</sup> and Gerard Meijer

*Department of Molecular and Laser Physics, Catholic University of Nijmegen, Toernooiveld 1, NL-6525 ED Nijmegen, The Netherlands*

(Received 23 May 1995; accepted 29 June 1995)

In a laser desorption jet-cooling molecular beam spectrometer the concentration of translationally and internally cooled laser desorbed organic molecules that can be achieved is experimentally determined. Sensitive direct absorption detection of laser desorbed jet-cooled diphenylamine (DPA) via cavity ring down (CRD) spectroscopy on the  $S_1 \leftarrow S_0$  transition around 308 nm is used to measure the line-integrated absolute absorption of the pulse of laser desorbed DPA molecules. The absolute cross section for the various vibrational bands of the electronic transition that is used, is determined in a separate two-color ionization experiment. It is concluded that the optimum beam intensity that is obtained with laser desorption is comparable to the beam intensity that is obtained in the same spectrometer by conventional seeding of the desired species at a partial pressure of  $10^{-4}$ . © 1995 American Institute of Physics.

## INTRODUCTION

Over the last decade laser desorption techniques have been applied in more and more sophisticated setups for mass-spectrometric sample characterization,<sup>1,2</sup> and a variety of laser desorption mass spectrometers are nowadays commercially available. When the advantages of laser desorption techniques are combined with the advantages of molecular beam techniques,<sup>3,4</sup> a versatile apparatus emerges that can be used both for mass-spectrometric sample analysis and for optical spectroscopic studies of internally cooled organic molecules that are hard to bring in the gas-phase otherwise.<sup>5-7</sup> It has been demonstrated by various groups that the detection sensitivity of such a laser desorption jet-cooling molecular beam spectrometer is such that femtograms of material are sufficient for a mass-spectrometric analysis, and that mass-resolved wavelength spectra can already be recorded using picograms of material.<sup>8</sup> In many cases, however, the amount of material that is available for spectroscopic characterization is not limited to picograms, and one would therefore like to know what the optimum beam intensity is that one can reach following the laser desorption approach. This beam intensity can then be compared to the typical beam intensities that one can reach when conventional seeding techniques are being used.

Here we report on the measurement of the concentration of "spectroscopic grade," i.e., translationally and internally cold, laser desorbed organic molecules that can be achieved in a laser desorption jet-cooling mass spectrometer. For this, the line integrated absolute absorption of a pulse of laser desorbed diphenyl-amine (DPA) molecules is measured in the collision-free part of the jet-expansion via cavity ring down (CRD) spectroscopy.<sup>9</sup> The absolute absorption cross section of the transitions that are used in the CRD measurements are determined in a separate two-color, two-photon ionization experiment. From the combined results of both measurements the line-integrated number density of DPA at a

known distance from the nozzle is accurately determined, and this result is then compared to the density that can be achieved in a conventional seeding experiment. DPA is used as a test molecule in this study, but the obtained value for the line-integrated number density is expected to be more generally valid; the optimum beam intensity of internally cooled laser desorbed molecules is rather molecule independent as it is mainly determined by the amount of laser desorbed material that can be allowed in front of the nozzle without a collapse of the molecular beam.

## EXPERIMENT

In Fig. 1 a scheme of the experimental setup is given. Gas pulses are released by a pulsed valve (Jordan Co., CA) with a 0.5 mm diam nozzle opening. The valve operates with 2 bar of Ar backing pressure at a 10 Hz repetition frequency and releases gas pulses of typically 30  $\mu$ s (FWHM) duration. In front of the nozzle a sample holder is mounted to which a 1 mm<sup>3</sup> piece of activated carbon, acting as a desorption matrix, saturated with diphenyl-amine (vapor pressure at room temperature around  $10^{-4}$  mbar) is attached. At the time that the peak intensity of the Ar carrier gas pulse is above the desorption matrix, the desorption laser is fired. For desorption, the unfocused frequency-doubled output of a Nd:YAG laser (approximately 1 mJ of 532 nm in a 1 mm diam spot;  $\approx 10^7$  W/cm<sup>2</sup>) is used. The use of activated carbon yields a stable source of DPA for many hours of operation.<sup>8,10</sup> Accurate positioning of the desorption substrate relative to the nozzle opening as well as accurate alignment of the desorption laser spot along the molecular beam axis is needed for optimum beam intensity. The laser desorbed molecules are entrained in the Ar gas pulse and are internally cooled by multiple collisions with the carrier gas atoms. This cooling process can be as efficient as in conventional seeding experiments provided the desorption takes place very close to the nozzle (within two nozzle diameters) and rotational temperatures down to 5 K have been demonstrated using this

<sup>a)</sup>E-mail: boog@sci.kun.nl

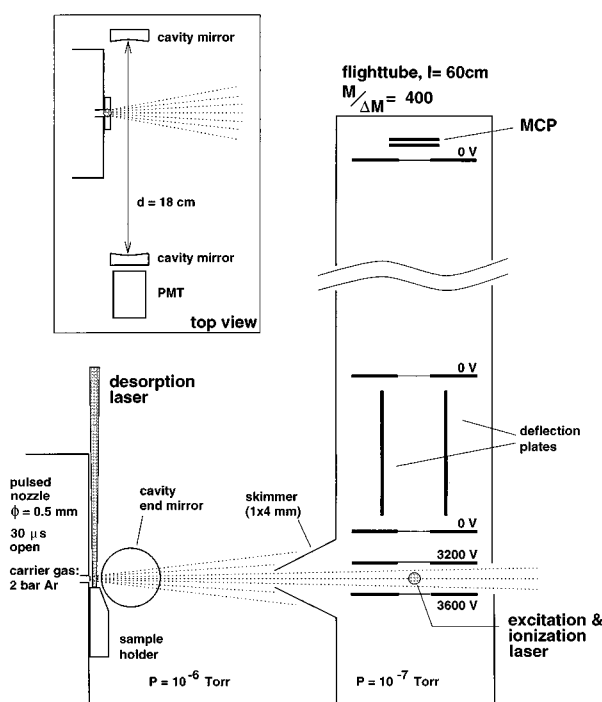


FIG. 1. Scheme of the experimental setup. A small portion of the laser beam that is used for REMPI of laser desorbed jet-cooled DPA in the ionization region is also used for the cavity ring down experiments that are performed closer to the nozzle. The length of the ring down cavity is chosen such that the CRD time matches to the spatial width of the DPA distribution, as described in the text.

approach.<sup>8</sup> The pulse of laser desorbed molecules travels along the molecular beam axis through the skimmer into the differentially pumped detection chamber.

In the region between the nozzle and the skimmer the laser desorbed molecules pass through an optical cavity in which the direct absorption measurements via cavity ring down (CRD) are performed.<sup>9</sup> The stable optical cavity is formed by two identical 25.4 mm diam plano-concave mirrors with a radius of curvature  $r = -25$  cm that are coated for an optimum reflectivity around 308 nm and that are placed 18 cm away from each other. The optical axis of the cavity is perpendicular to the molecular beam axis and intersects the molecular beam at a distance from the nozzle varying from 5 mm up to 20 mm. In the spectral region of interest for this study (305–310 nm) the mirrors have a reflectivity  $R$  of around 99.6%.

In the differentially pumped detection chamber the molecular beam enters the region between the extraction plates of a linear time-of-flight (TOF) setup, where it is intersected perpendicularly with the counterpropagating beams of a pulsed tunable dye laser and a broadband ArF (193 nm) excimer laser. Tunable pulsed radiation in the 305–310 nm range is obtained via frequency doubling the output of a dye laser pumped by the second harmonic of a Nd:YAG laser (Spectra Physics GCR 150/PDL-3/WEX combination). Typically up to 5 mJ of tunable radiation with a bandwidth of  $0.15 \text{ cm}^{-1}$  is obtained.

As indicated schematically in Fig. 2, (1+1)-resonance enhanced multiphoton ionization can be performed on DPA

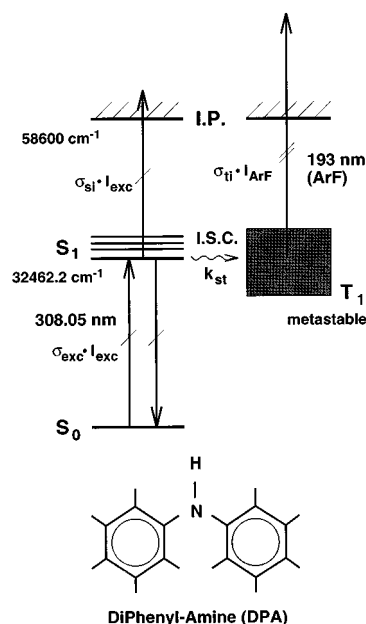


FIG. 2. Schematic representation of the diphenylamine (DPA) molecule and of the excitation and ionization schemes that are relevant for this study. The various parameters that are used in the theoretical modeling of the measured saturation curves are indicated.

using this dye laser radiation. The ions produced in this process are mass selectively detected in a Wiley–McLaren TOF setup. At low laser fluence ( $\leq 1.0 \text{ mJ/cm}^2$ ) the parent ion of DPA (mass 169) as well as of its <sup>13</sup>C isotope are the only ions observed. With a flight path of 60 cm a mass resolution of  $M/\Delta M = 400$  is obtained. The ion signal is detected by a dual MCP detector, amplified and displayed on a digital oscilloscope with a 10 ns sampling time and a 10 bit vertical resolution (LeCroy 9430). The data from the oscilloscope is read into a PC via a GPIB interface where they are further manipulated and displayed. The PC also controls the scanning of the dye laser as well as the settings of the digital delay generators (Stanford Research DG535).

Due to a rapid intersystem crossing (ISC), the lifetime of the  $S_1$  state of DPA is rather short. By scanning the time delay between the excitation laser and another Nd:YAG pumped ionization laser in a two-color (1+1)-REMPI scheme, we were not able to determine an accurate value for the  $S_1$  lifetime of DPA, and concluded on an upper limit of the  $S_1$ -state lifetime of 5 ns.<sup>10</sup> In solution a value of 3 ns has been determined for the fluorescence lifetime of singlet excited DPA.<sup>11,12</sup> After intersystem crossing, the long-lived triplet states of DPA can be detected using an ArF excimer laser (193 nm; 6.42 eV) for (time-delayed) ionization out of the triplet manifold.

In the upper part of Fig. 3 both the one color (1+1)-REMPI spectrum and the two-color (1+1)-REMPI spectrum of laser desorbed jet-cooled DPA measured on the mass of the parent ion are shown. The spectra are corrected for laser intensity fluctuations and are measured under such conditions that saturation effects are unimportant. Long progressions in a torsional mode ( $62.5 \text{ cm}^{-1}$ ) and in a wagging

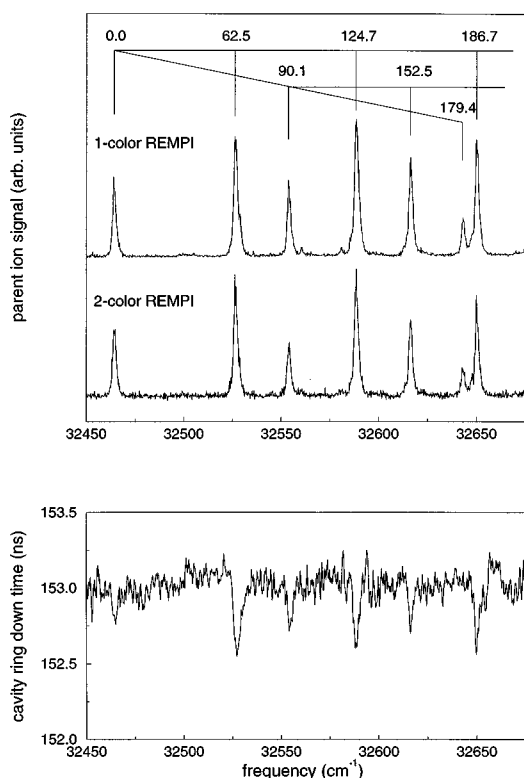


FIG. 3. Upper panel: One color (1+1)-REMPI spectrum and two-color (1+1)-REMPI spectrum of laser desorbed jet-cooled DPA measured on the mass of the parent ion. In the two-color REMPI spectrum the ArF ionization laser is delayed 150 ns relative to the excitation laser, and ionization is performed out of the triplet manifold after rapid intersystem-crossing. Lower panel: Cavity ring down absorption spectrum recorded at a distance of 11 mm away from the nozzle under otherwise identical conditions.

mode ( $90.1 \text{ cm}^{-1}$ ) of the phenyl rings as well as their combination bands are observed in the spectra. In the two-color REMPI spectrum the ArF ionization laser is delayed 150 ns relative to the excitation laser, and ionization is performed out of the triplet manifold after rapid intersystem crossing. It is noted that the ions produced via one-color (1+1)-REMPI of the dye laser and those produced via two-color (1+1)-REMPI via the combination of the dye laser and the excimer laser can be measured simultaneously as both groups of  $\text{DPA}^+$  ions arrive at the detector with a 150 ns time separation. From the close agreement between the REMPI spectra measured via the two distinctly different pathways it is concluded that in the spectral region up to a few hundred  $\text{cm}^{-1}$  above the vibrationless level in the  $S_1$  state of DPA, the intersystem crossing rate is not vibrational-mode selective.

### CRD DETECTION OF DPA

A small fraction of the pulsed dye laser beam that is used for resonant excitation and ionization of DPA is split off after exiting the molecular beam machine, and is coupled into the ring down cavity for the measurement of the direct absorption of the jet-cooled DPA molecules. Typically, on the order of  $1 \mu\text{J}$  of tunable radiation in a 2 mm diam spot is directed toward the cavity, and only a small fraction of this (on the order of  $10^{-3}$ ) is coupled into the cavity through the highly

reflecting mirror. The time dependence of the light intensity in the stable optical cavity is monitored via detection of the light that is leaking out through the other mirror with a photomultiplier placed closely behind the outcoupling mirror, outside the molecular beam machine. Using the same laser beam in the ionization region and in the ring down cavity has the advantage that all experimental parameters can be optimized using the most sensitive detection scheme, i.e., the REMPI scheme. A similar combination of ionization and CRD detection schemes has recently been applied by Saykally and co-workers in their study of copper silicides.<sup>13</sup> In switching from REMPI detection to CRD detection of DPA only the timing of the dye laser relative to the desorption laser has to be changed, and this by an amount that can be accurately estimated.

If a monochromatic light pulse at frequency  $\nu$  is coupled into an otherwise empty cavity, the ring down transient  $I_{\text{CRD}}(t)$  is a single exponentially decaying function of time with a  $1/e$  "cavity ring down time"  $\tau(\nu)$  which is solely determined by the reflectivity  $R(\nu)$  of the mirrors and the optical pathlength  $d$  between the mirrors. The presence of absorbing species in the ring down cavity can now be deduced from a resulting decrease in the cavity ring down time. It follows, therefore, that in the more general case  $I_{\text{CRD}}(t)$  is proportional to

$$I_{\text{CRD}}(t) \propto \int_0^\infty I(\nu) e^{-t/\tau(\nu)} d\nu, \quad (1)$$

where  $\tau(\nu)$  is given by

$$\tau(\nu) = \frac{d}{c[|\ln(R(\nu))| + \sum_i \sigma_i(\nu) \int_0^d N_i(x) dx]} \quad (2)$$

and the sum is over all light scattering and absorbing species with frequency-dependent cross sections  $\sigma_i(\nu)$  and a line-integrated number density  $\int_0^d N_i(x) dx$ .<sup>9,14,15</sup>

With the cavity designed as described above, the cavity mode spectrum is quasicontinuous<sup>16</sup> due to the lifting of the degeneracy of the longitudinal and transverse modes. As long as the laser linewidth is spectrally narrower than the absorption feature of the species under study, the time dependence of the light intensity inside the cavity is correctly described with a single exponentially decaying curve.<sup>15,17</sup> It is noted once more, that in a CRD experiment the rate of absorption of a light pulse confined in a closed optical cavity is measured and the measurement is therefore independent of light source intensity fluctuations, as long as the spectral intensity distribution of the light stays constant from pulse to pulse. The ring down transient is displayed on the same digital oscilloscope, and averaged over typically 25 laser pulses. The averaged signal is read in by the PC and the characteristic ring down time is determined by fitting the natural logarithm of the data to a straight line, using a weighed least-squares fitting algorithm. The time constant that describes the decay of the empty cavity in our setup is around 150 ns, and the exact value of the lifetime can be determined to an accuracy better than  $10^{-3}$ , implying a noise-equivalent absorption detection limit below 4 ppm per pass. It is noted that in the description of the CRD experiment given here, it is

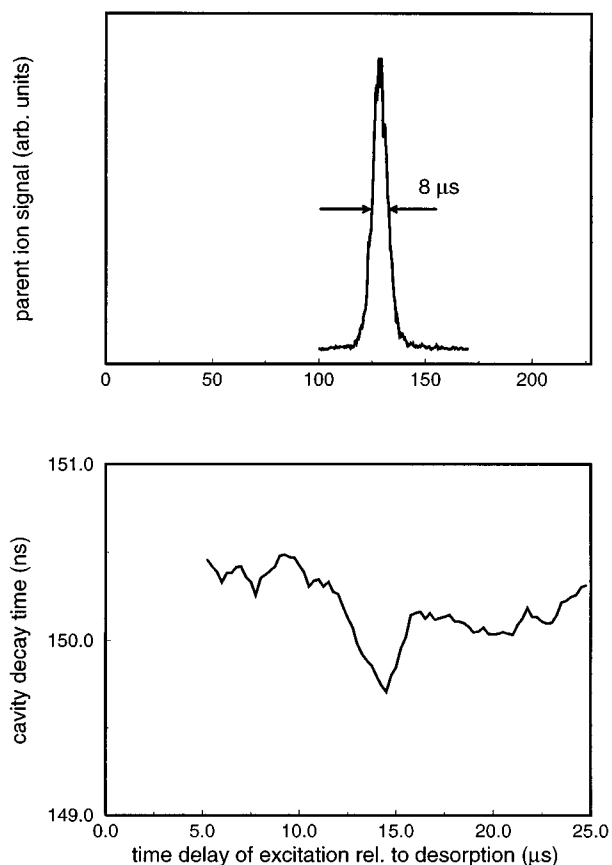


FIG. 4. Time-of-flight distributions of neutral laser desorbed jet-cooled DPA molecules detected via (i) REMPI with parent ion detection at a distance of 10 cm from the nozzle (upper panel), and (ii) cavity ring down (CRD) absorption at a distance of 11 mm from the nozzle (lower panel).

assumed that the density of absorbing species is constant during the measurement time, which in our case amounts to approximately 500 ns.

In the upper part of Fig. 4 the time-of-flight distribution of laser desorbed jet-cooled DPA in Ar as measured in the ionization region via one-color (1+1)-REMPI on the origin of the  $S_1 \leftarrow S_0$  transition at  $32\,462.2\text{ cm}^{-1}$  is shown. On the horizontal axis the time delay of the excitation laser relative to the desorption laser is indicated. As the distance between the nozzle and the center of the ionization region is 10 cm, the most probable velocity of the DPA is  $760 \pm 25\text{ m/s}$ . This is somewhat higher than the expected velocity of Ar expanding from a reservoir at room temperature, implying that the actual temperature of the expanding gas is slightly above room temperature in this kind of pulsed valve, an observation that has also been reported by others.<sup>18</sup> It is noted that the width of the velocity distribution corresponds to a translational temperature of 2.0 K, and to a length of the jet-cooled DPA pulse in the ionization region of 6 mm.

Under otherwise identical experimental conditions, the CRD time has been measured as a function of the time delay between the desorption laser and the dye laser, and is shown in the lower part of Fig. 4. As the optical axis of the ring down cavity intersects the molecular beam axis 11 mm downstream from the nozzle, the cloud of jet-cooled DPA is expected to be in the cavity after approximately 14  $\mu\text{s}$ , and

exactly around this time a slight decrease in CRD time is observed. In Fig. 4 both time-of-flight distributions are shown on a horizontal axis that is scaled relative to the distance of the measurement point to the desorption point, and there clearly is a good agreement. The size of the laser beam in the cavity is on the order of 0.5 mm whereas the “length” of the pulse of DPA is only slightly longer, so the relative width of the lower TOF distribution in Fig. 4 is expected to be larger than the one shown in the upper panel. It is noted that with the cavity length as chosen, the total time interval during which the CRD transient is measured is matched well to the time that the pulse of DPA spends in the cavity. Attention is drawn to the vertical scale in the lower figure; a maximum decrease of 0.4 ns, corresponding to an absorption per pass of 11 ppm, is observed.

With the time delay between the dye laser and the desorption laser fixed at the value where the largest decrease in CRD time is observed, i.e., around 14  $\mu\text{s}$ , a wavelength scan is made with the dye laser to unambiguously demonstrate that jet-cooled DPA is indeed responsible for the observed decrease in CRD time. The absorption spectrum thus obtained is shown in the lower part of Fig. 3, and all peaks observed match well to the REMPI spectra displayed in the upper panel of the same figure. On the strongest line the relative decrease in CRD time is on the order of  $(4 \pm 1)10^{-3}$ . As the decay time of 153 ns for the 18 cm long empty cavity implies an effective mirror reflectivity  $R=0.9961$ , it is concluded that the maximum line integrated peak absorption  $\sigma(\nu) \int_0^d N_{\text{DPA}}(x) dx$  is  $(16 \pm 4)$  ppm per pass.

## ABSOLUTE CROSS-SECTION MEASUREMENTS

To be able to extract an absolute number density of DPA molecules from the measured direct absorption spectrum as shown in the lower panel of Fig. 3, the absolute value for the excitation cross section of DPA needs to be known. This value can be determined by measuring the excitation efficiency on the various vibrational bands of the  $S_1 \leftarrow S_0$  transition of DPA as a function of a calibrated photon fluence, i.e., by measuring the saturation curve of the  $S_1 \leftarrow S_0$  transition.<sup>19–21</sup> In principle, this can be done in a one-color (1+1)-REMPI scheme where one expects a quadratic laser fluence dependence that changes into a linear one and eventually saturates with increasing laser fluence. It is important to measure the total ion intensity in this process, as for high laser fluences severe fragmentation of the parent ion will occur. The absorption cross section can be determined more accurately in the time-delayed two-color (1+1)-REMPI setup in which ionization is performed via the triplet manifold after intersystem crossing. In this latter scheme, the intensity of the ionization laser can be kept fixed at a value where fragmentation does not yet occur, and the parent ion intensity is measured as a function of the calibrated fluence of the excitation laser. In addition, the excitation and ionization processes are now separated in time, and (unwanted) coherence effects are largely avoided. The saturation curve will now simply change from linear to a saturated, laser fluence independent, behavior when the excitation laser inten-

sity is increased, as long as competing ionization from the excited singlet state with the excitation laser can be neglected.

In the rate-equation approach, which is applicable in this case as the lasers employed have a rather large bandwidth and the lifetime of the excited state of DPA is relatively short, the following set of differential equations has to be solved:

$$\begin{pmatrix} \frac{dn_{S_0}}{dt} \\ \frac{dn_{S_1}}{dt} \\ \frac{dn_{T_1}}{dt} \\ \frac{dn_{I_S}}{dt} \end{pmatrix} = \begin{pmatrix} -\sigma_{\text{exc}}I_{\text{exc}} & \sigma_{\text{exc}}I_{\text{exc}} & 0 & 0 \\ \sigma_{\text{exc}}I_{\text{exc}} & -(\sigma_{\text{exc}}I_{\text{exc}} + k_{\text{st}} + \sigma_{\text{si}}I_{\text{exc}}) & 0 & 0 \\ 0 & k_{\text{st}} & 0 & 0 \\ 0 & \sigma_{\text{si}}I_{\text{exc}} & 0 & 0 \end{pmatrix} \times \begin{pmatrix} n_{S_0}(t) \\ n_{S_1}(t) \\ n_{T_1}(t) \\ n_{I_S}(t) \end{pmatrix}. \quad (3)$$

In these equations  $n_{S_0}$ ,  $n_{S_1}$ ,  $n_{T_1}$ , and  $n_{I_S}$  are the number densities of DPA molecules in the electronic ground state, in the excited singlet state, in the triplet manifold and the number of ions produced via the excited singlet state in a one-color (1+1)-REMPI scheme, respectively. The various cross sections and excitation fluences together with the intersystem crossing rate  $k_{\text{st}}$  are indicated in Fig. 2. As prior to the excitation laser pulse all the population is in the electronic ground state [ $n_{S_0}(t=0) = N_{\text{DPA}}$ ], the population in the triplet manifold ( $n_{T_1}$ ) and the number of ions produced in a one-color (1+1)-REMPI scheme via the excited singlet state ( $n_{I_S}$ ) at the end of the dye laser pulse (at  $t = T$ ) can be written as

$$n_{T_1}(T) = \frac{k_{\text{st}}}{k_{\text{st}} + \sigma_{\text{si}}I_{\text{exc}}} \left[ \frac{\lambda_+}{\lambda_+ - \lambda_-} (1 - e^{-\lambda_- T}) - \frac{\lambda_-}{\lambda_+ - \lambda_-} (1 - e^{-\lambda_+ T}) \right] N_{\text{DPA}}, \quad (4)$$

$$n_{I_S}(T) = \frac{\sigma_{\text{si}}I_{\text{exc}}}{k_{\text{st}}} n_{T_1}(T), \quad (5)$$

where  $\lambda_{\pm}$  are defined as

$$\lambda_{\pm} = - \left[ \sigma_{\text{exc}}I_{\text{exc}} + \frac{1}{2}(k_{\text{st}} + \sigma_{\text{si}}I_{\text{exc}}) \right] \pm \sqrt{(\sigma_{\text{exc}}I_{\text{exc}})^2 + \left(\frac{1}{2}(k_{\text{st}} + \sigma_{\text{si}}I_{\text{exc}})\right)^2}. \quad (6)$$

In the one-color (1+1)-REMPI scheme the quantity  $n_{I_S}(T)$  is measured, whereas in the two-color time-delayed (1+1)-REMPI detection scheme the number of ions produced via the triplet manifold with the ArF ionization laser is measured. The latter quantity is directly proportional to  $n_{T_1}(T)$ , with the proportionality constant determined by the laser fluence of the ArF laser and the cross section for single-photon ionization out of the triplet manifold.

In Fig. 5 a measurement of the total ion yield, i.e., all fragment ions are detected as well, of DPA via either ioniza-

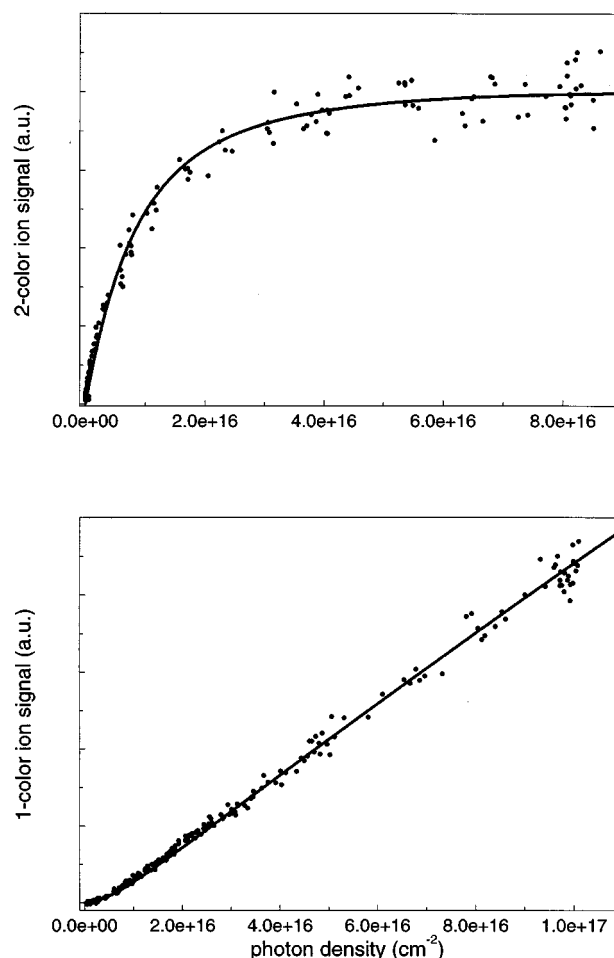


FIG. 5. Experimentally measured and fitted saturation curves employing either time-delayed (300 ns) ionization with the ArF laser from the triplet manifold (upper panel) or direct ionization out of the excited singlet state with the same laser that is used for resonant excitation (lower panel).

tion pathway is given as a function of the fluence of the resonant excitation laser. The laser is kept fixed in wavelength on the electronic origin of the  $S_1 \leftarrow S_0$  transition. The total ion yield averaged over 20 laser shots is measured simultaneously with the averaged excitation laser fluence. The latter is measured on a relative scale with a photomultiplier tube, and only afterward put on an absolute scale by measuring the laser power with a calibrated power meter. In this measurement only the central 1.0 mm diam portion of the excitation laser beam is coupled into the molecular beam machine through a well-defined mask; the spatial intensity distribution over this 1.0 mm diam area varies less than 20%. The beam size of the ArF ionization laser is chosen somewhat larger than that of the excitation laser. The intensity of the ArF laser is attenuated using a variable filter to such an extent that the two-photon nonresonant ionization of ground-state DPA that it can induce is not detectable any longer.

The data given in Fig. 5 are fitted to the expressions described above. Compared to the intersystem-crossing rate  $k_{\text{st}}$  the ionization out of the singlet state with the excitation laser, i.e.,  $\sigma_{\text{si}}I_{\text{exc}}$ , appears to be only a minor loss channel, even up to the highest excitation laser fluences that have

been used. This is most directly seen in the upper panel of Fig. 5; if the ionization out of the singlet state would compete with the intersystem crossing rate, the measured curve would bend downward for high laser fluences but instead it remains more or less flat. It turned out to be impossible to fit all three unknown parameters,  $\sigma_{\text{exc}}$ ,  $k_{\text{st}}$ , and  $\sigma_{\text{si}}$ , simultaneously. Best agreement with the experimental results is obtained when  $k_{\text{st}}$  is set equal to  $3 \times 10^8 \text{ s}^{-1}$  (corresponding to an excited state lifetime of around 3 ns). The resonant excitation cross section can be rather accurately determined as  $\sigma_{\text{exc}} = (1.1 \pm 0.2) \times 10^{-16} \text{ cm}^2$ , whereas an upper limit for the cross section for ionization out of the singlet state is determined as  $\sigma_{\text{si}} \leq 5 \times 10^{-18} \text{ cm}^2$ . The latter value for the ionization cross section implies that even at the largest laser fluences employed, the product  $\sigma_{\text{si}} I_{\text{exc}}$  is less than  $0.3 k_{\text{st}}$ . The correctly scaled fit thus obtained is shown together with the measurements in both panels of Fig. 5. Similar measurements have been performed for all the vibrational bands that are shown in the spectra of Fig. 3, and the relative intensity of the absolute values for the excitation cross sections determined for these bands match well to the intensity distribution as shown in the REMPI spectra. The vibrational band that showed an absorption of  $(16 \pm 4)$  ppm per pass in the CRD measurements is determined to have a peak absorption cross section  $\sigma_{\text{exc}}$  of  $(1.6 \pm 0.3) \times 10^{-16} \text{ cm}^2$ .

## CONCLUSIONS

Sensitive direct absorption measurements have been performed on laser desorbed diphenyl-amine just outside the expansion region of a molecular beam machine via cavity ring down spectroscopy. Even at CRD times as short as 150 ns, a noise-equivalent absorption detection limit below 4 ppm per pass has been demonstrated in the near UV part of the spectrum around 308 nm. The strongest vibrational band of the  $S_1 \leftarrow S_0$  transition of DPA shows an absorption of  $(16 \pm 4)$  ppm at a distance of 11 mm (22 nozzle diameters) from the nozzle. In a two-color time-delayed (1+1)-REMPI scheme the absolute absorption cross section for the same vibrational band has been determined as  $(1.6 \pm 0.3) \times 10^{-16} \text{ cm}^2$ . Combining these results leads to a value for the line-integrated DPA number density inside the ring down cavity of  $\int_0^d N_{\text{DPA}}(x) dx = (1.0 \pm 0.25) \times 10^{11} \text{ cm}^{-3} \text{ cm}$ . To extract the absolute number density of DPA inside the ring down cavity from these combined measurements, the length of the absorption path needs to be known.

Measurement of spatial distributions of laser desorbed species in a molecular beam has been performed by Arrow-smith *et al.*,<sup>22</sup> albeit that the experimental conditions were not optimized for optimum cooling conditions and a different pulsed valve from the one we employed was used. Their results will nevertheless be largely applicable to our system, and from these measurements we estimate a FWHM spatial distribution of DPA of 3 mm at 22 nozzle diameters away from the desorption point. We can now approximate the in-

tegral along a line with a varying DPA concentration by an averaged DPA concentration times a 3 mm width of the DPA package. This then results in an approximate DPA number density on the axis of the molecular beam machine at an 11 mm distance from the nozzle of  $N_{\text{DPA}} \approx 3 \times 10^{11} \text{ cm}^{-3}$ . This number density is estimated to be correct within a factor of 2.

This number density can be compared to the number density that can be reached in a conventional seeding experiment,<sup>4</sup> and it is concluded that the on-axis beam intensity is comparable to seeding a molecule in the same beam machine at a partial pressure of  $10^{-4}$ , i.e., it is comparable to the situation in which a molecule with a vapor pressure of 0.1 mbar is seeded in 1 bar of Ar. It is indeed experimentally observed that seeding aniline, which has a 0.4 mbar vapor pressure at room temperature but also a factor four smaller excitation cross section<sup>20</sup> than DPA, in 1 bar Ar in the same beam machine results in spectra of comparable intensity as observed for laser desorbed DPA.

## ACKNOWLEDGMENTS

This work is part of the research program of the "Stichting voor Fundamenteel Onderzoek der Materie (FOM)," and is financially supported by the "Nederlandse Organisatie voor Wetenschappelijk Onderzoek (NWO)."

- <sup>1</sup>M. A. Posthumus, P. G. Kistemaker, H. L. C. Meuzelaar, and M. C. ten Noever de Brauw, *Anal. Chem.* **50**, 985 (1978).
- <sup>2</sup>J. H. Hahn, R. Zenobi, J. L. Bada, and R. N. Zare, *Science* **239**, 1523 (1988).
- <sup>3</sup>D. H. Levy, *Science* **214**, 263 (1981).
- <sup>4</sup>*Atomic and Molecular Beam Methods*, edited by G. Scoles (Oxford University, Oxford, 1988).
- <sup>5</sup>J. R. Cable, M. J. Tubergen, and D. H. Levy, *J. Am. Chem. Soc.* **109**, 6198 (1987).
- <sup>6</sup>J. Grotemeyer and E. W. Schlag, *Angew. Chem. Int. Ed. Engl.* (27), 447 (1988).
- <sup>7</sup>*Lasers and Mass Spectrometry*, edited by D. M. Lubman (Oxford University, Oxford, 1990).
- <sup>8</sup>G. Meijer, M. S. de Vries, H. E. Hunziker, and H. R. Wendt, *Appl. Phys. B* **51**, 395 (1990).
- <sup>9</sup>A. O'Keefe and D. A. G. Deacon, *Rev. Sci. Instrum.* **59**, 2544 (1988).
- <sup>10</sup>M. G. H. Boogaarts, P. C. Hinnen, and G. Meijer, *Chem. Phys. Lett.* **223**, 537 (1994).
- <sup>11</sup>H. J. Haink and J. R. Huber, *Chem. Phys. Lett.* **74**, 117 (1976).
- <sup>12</sup>R. Rahn, J. Schroeder, J. Troe, and K. H. Grellmann, *J. Phys. Chem.* **93**, 7841 (1989).
- <sup>13</sup>J. J. Scherer, J. B. Paul, C. P. Collier, and R. J. Saykally, *J. Chem. Phys.* **102**, 5190 (1995).
- <sup>14</sup>D. Romanini and K. K. Lehmann, *J. Chem. Phys.* **99**, 6287 (1993).
- <sup>15</sup>R. T. Jongma, M. G. H. Boogaarts, I. Holleman, and G. Meijer, *Rev. Sci. Instrum.* **66**, 2821 (1995).
- <sup>16</sup>G. Meijer, M. G. H. Boogaarts, R. T. Jongma, D. H. Parker, and A. M. Wodtke, *Chem. Phys. Lett.* **217**, 112 (1994).
- <sup>17</sup>P. Zalicki and R. N. Zare, *J. Chem. Phys.* **102**, 2708 (1995).
- <sup>18</sup>H. Meyer, *J. Chem. Phys.* **101**, 6686 (1994).
- <sup>19</sup>D. S. Zakheim and P. H. Johnson, *Chem. Phys.* **46**, 263 (1980).
- <sup>20</sup>U. Boesl, H. J. Neusser, and E. W. Schlag, *Chem. Phys.* **55**, 193 (1981).
- <sup>21</sup>H. Zacharias, R. Schmiedl, and K. H. Welge, *Appl. Phys.* **21**, 127 (1980).
- <sup>22</sup>P. Arrowsmith, M. S. de Vries, H. E. Hunziker, and H. R. Wendt, *Appl. Phys. B* **46**, 165 (1988).